Journal of Power Electronics
https://doi.org/10.1007/s43236-025-01102-5

ORIGINAL ARTICLE

Randomly modulated spread spectrum technique employed in boost PFC circuits

Young-Joon Song[1] · Kyung-Wook Heo[2] · Jun-Suk Lee[1] · Sang-Yeop Kim[1] · Jee-Hoon Jung[1]

Received: 8 March 2025 / Revised: 8 June 2025 / Accepted: 11 June 2025

Abstract
Boost power factor correction (PFC) circuit is widely employed in industrial applications to provide regulated DC-link voltage and high-power factor. However, the high switching frequency in boost PFC circuit generates significant electromagnetic (EM) noise. Although electromagnetic interference (EMI) filters can effectively mitigate EM noises, they introduce trade-offs, such as high cost, low efficiency, and low power density. To address those challenges, spread spectrum modulation (SSM) methods have been researched. They distribute the switching frequency over a wide frequency band, reducing peak and quasi-peak EM noises. Random SSM shows high EM noise mitigation performance due to its ability to uniformly distribute noise in a stochastic manner. However, random SSM increases computational burden due to random number generation and operating instability from abrupt frequency shifts in power converters. Although employing random SSM in a CCM boost PFC can effectively mitigate EM noise, its control performance cannot be guaranteed due to distorted current sampling data. To overcome those drawbacks, this paper proposes a variable sampling method to implement random SSM under CCM boost PFC circuit. The design methodology of the proposed random SSM for the boost PFC circuit, focusing on digital implementation, EMI reduction. In addition, associated side effects according to various SSM parameters are analyzed and discussed.

Keywords Power factor correction · Spread spectrum modulation · Electromagnetic interference · Random modulation · Variable sampling

1 Introduction

Boost power factor correction (PFC) circuits have been widely employed in industries to meet electromagnetic compatibility (EMC) standards [1–3]. Among the three modes of the PFC operations, the continuous conduction mode (CCM) is frequently chosen for high-power applications due to its reduced current ripple and low total harmonic distortion (THD). However, although boost PFC circuit improve harmonic compliance, it also generate EM noise, complicating compliance with EMI regulations.

The EM noise in the boost PFC circuit typically manifests as differential mode (DM) noise, which arises from inductor current ripples, and common mode (CM) noise induced by parasitic capacitances [4]. Various approaches have been introduced to mitigate the EM noise, such as shielding, groundings, PCB layout changes, and passive EMI filters [5–10]. However, achieving regulatory compliance often requires multiple stages of the passive EMI filters, which increases manufacturing costs and reduces power density.

Spread spectrum modulation (SSM) has emerged as a promising strategy to alleviate the burden on passive EMI filters by varying the switching frequency of the PFC circuit using periodic and random modulation patterns [11, 12]. Rather than concentrating the EM noise at a single switching frequency, the SSM disperses the noise energy across a wide frequency band, reducing its peak and quasi-peak values.

Nonetheless, the SSM introduces specific side effects. Various research has been conducted to optimize EM noise mitigation performance while minimizing the side effects of the SSM in the power stage. In [13], SSM was applied to flyback PFC operating in the discontinuous conduction mode (DCM). When SSM was employed, current distortion occurred on the input side due to the switching frequency

✉ Jee-Hoon Jung
jhjung@unist.ac.kr; jung.jeehoon@gmail.com

[1] Department of Electrical Engineering, Ulsan National Institute of Science and Technology (UNIST), Ulsan, Republic of Korea

[2] Agency for Defense Development (ADD), Daejeon, Republic of Korea

Published online: 28 June 2025

term in the input current, degrading power factor (PF) by increasing inductor current ripple. By employing a small-signal model to analyze the effects of SSM, the author adjusted SSM with additional dead time to minimize its effect on input current. The given method showed 14 dB of reduced EM noise with a 2.9% THD decrease compared with conventional fixed-mode operation. In [14], SSM was employed in a three-level boost PFC operating in the DCM.

Since DM noise is proportional to inductor current ripple, minimizing the current ripple on the inductor can reduce DM noise while reducing the current stress of devices. The author proposed an adaptive three-level current, adding an adaptive single-switch on-time t_α in each switching cycle to obtain three-level current modulation. Compared to conventional SSM, the method reduced an additional 2.7 dB of DM noise.

Despite extensive research on SSM in DCM PFC, application to boost PFC operating in CCM using random SSM has not been thoroughly investigated. Previous studies [13, 14] have implemented SSM in DCM PFC using only an outer voltage loop. A common limitation of these studies is that SSM has not been directly used in converter employing current control. In CCM boost PFC, current control is essential to shape the current reference sinusoidally and keep it in phase with the input voltage. However, random SSM can adversely affect converter performance due to abrupt switching frequency changes and discrepancies between the sampled current and the actual average current.

This study proposes a random SSM implemented in a 1.4 kW boost PFC prototype using average current mode control, aiming to address the above technical challenges. The performance of the proposed random SSM is systematically evaluated by examining the trade-offs among EM noise mitigation, THD, and efficiency. By employing a variable sampling method to implement random SSM in average current mode control, sample data errors relative to the actual average current can be minimized. This enables effective EM noise mitigation while preserving input current waveform quality. Furthermore, a detailed examination for implementing the proposed random function algorithm is presented with suitable experimental results.

2 Random SSM in boost PFC

2.1 Technical background of SSM

Figure 1 illustrates spectral waveforms with and without the SSM, where f_c represents the center frequency and Δf denotes the amplitude of frequency variations. By modulating the switching frequency across a range of $2\Delta f$, the EM noise is distributed across a wider bandwidth as follows:

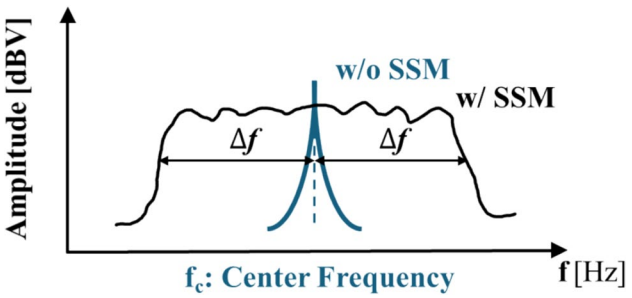

Fig. 1 Conceptual EM noise distributions with and without SSM

$$s(t) = A_0\left(2\pi f_c t + 2\pi\Delta f \int_{-\infty}^{t} \xi(\tau)d\tau\right) \quad (1)$$

where $s(t)$ is the frequency modulation signal, A_0 is the amplitude of the switching signal, and $\xi(\tau)$is the modulation pattern of the SSM varying between -1 to 1 with a period of $1/f_m$ [15]. According to Carson's rule, the power of $s(t)$ is $A_0^2/2$, which is equivalent to operating at a fixed frequency. However, power disperses within Carson's bandwidth [f_c–Δf, $f_c + \Delta f$], reducing the peak value.

The SSM is categorized into two types: periodic SSM and random SSM. Periodic SSM refers to a modulation scheme with a periodic switching pattern, which facilitates straightforward implementation and minimizes the computational demands. It allows for predictable performance assessment through the modulation index ($m_f = \Delta f/f_m$) directly correlating with EM noise mitigation. In contrast, random SSM employs switching patterns that change randomly. Random SSM can be further categorized based on the method used to implement the random numbers [16]. A widely known method is pseudo-random modulation. As depicted in Fig. 2, pseudo-random modulation maintains a constant f_m. However, the magnitude of the switching frequency varies between the limited values. Random SSM can also be expressed in mitigation performance with m_f, as depicted in Fig. 3. Compared with periodic SSM, it shows higher mitigation performance under the same m_f but lacks accuracy [17].

However, random SSM has side effects when employed in power converters. Generating a random value in every f_m

can be challenging due to the use of complex algorithms. In addition, abrupt frequency transitions can introduce instability in power converters. Despite those shortcomings, the random SSM has the advantage of EM noise mitigation performance. Due to its randomness, it enables more uniformly distributed noise across the bandwidth, enhancing the EM noise mitigation performance compared with periodic SSM.

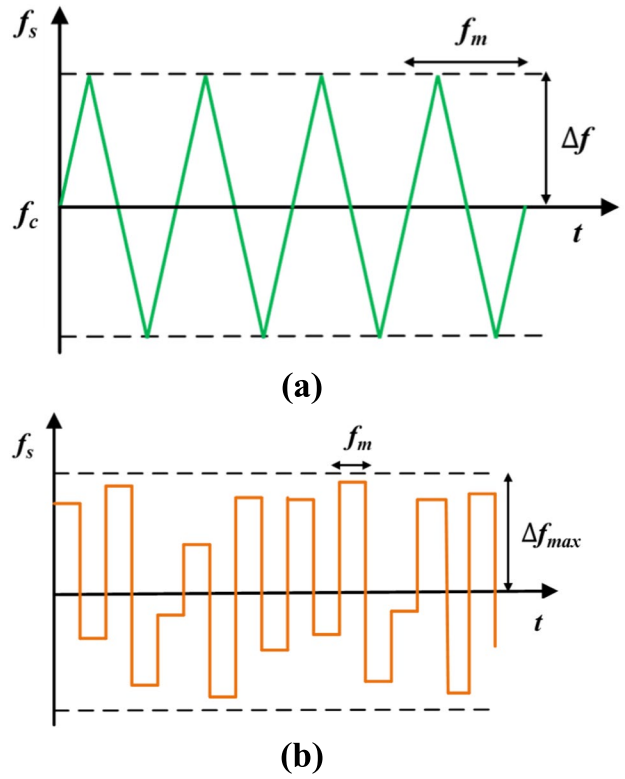

Fig. 2 Spread spectrum modulation (SSM): **a** periodic; **b** random (pseudo-random modulation)

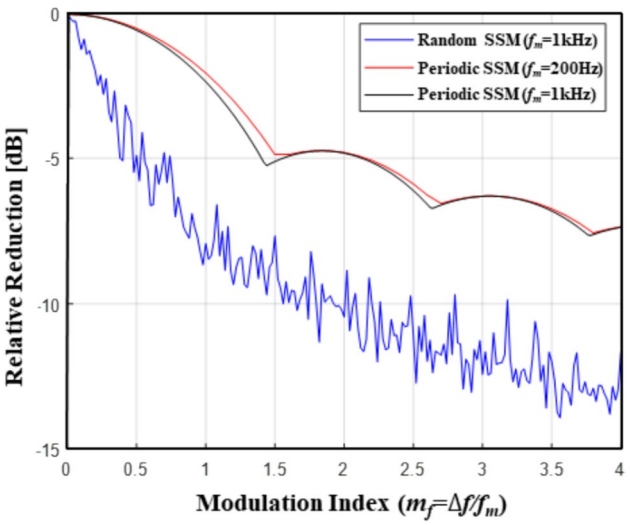

Fig. 3 EM noise mitigation performance versus modulation index

2.2 Impact of random SSM on a boost PFC circuit

While employing SSM in a boost PFC circuit to mitigate EM noise, the impact varies depending on the operating region. When the boost PFC is designed to operate in the DCM, the input current can be shown as below [18]:

$$i_{in\_avg}(t) = \frac{D^2 V_o v_{in}(t)}{2L_B[V_o - v_{in}(t)]f_s(t)} \tag{2}$$

where $v_{in}(t)$ is the input voltage, V_o denotes the output voltage, L_B indicates the boost inductance, D is the duty cycle, and $f_s(t)$ is the switching frequency employing SSM. The controller regulates D to compensate for variations of f_s. However, the voltage controller in the PFC is designed with a cutoff frequency between 10 ~ 30 Hz, which makes it difficult for the voltage controller to compensate for output voltage fluctuations. Therefore, the input current spectrum includes interharmonic components of $f_m \pm f_{grid}$, which degrades the PFC performance [13].

However, when the boost PFC circuit operates in the CCM, the DCM region only occupies a small portion of the cycle, reducing the impact of the switching frequency on the input current. The reference of the input current is defined as (3) when using average current mode control as follows:

$$i_{L\_ref} = \frac{G_v|v_{in}(t)|}{V_{in}^2} \tag{3}$$

where G_v represents the output of the outer voltage loop, and V_{in} denotes the rms value of the input voltage. Since the reference of the input current does not need to compensate for terms related to $f_s(t)$, the current controller can regulate the switching current following the reference current. Therefore, for the CCM boost PFC circuit, employing SSM has merits compared with the DCM.

However, in the average current mode control, it is crucial for the sampled current to represent the average value for every switching cycle to obtain high PF and low THD. The conventional fixed sampling method can lead to a discrepancy in the CCM between the sampled current and the actual average current, resulting in switching current distortions.

3 Design methodology

3.1 Variable sampling technique for average current mode control

Figure 4 shows the average current mode control with random SSM in the boost PFC. It uses the sensed input voltage multiplied by the voltage loop compensator. Then, their product is divided by the square of the RMS value of the input voltage, resulting in the input current reference. The regulator compensates for the error between the current reference and the sensed current, which is sampled periodically. The output of the current compensator is compared with triangular waveforms to generate the gating signals in the PWM process (Fig. 5).

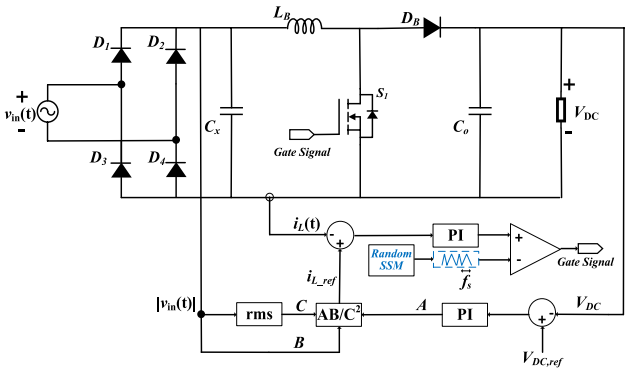

Fig. 4 Functional diagram of average current mode control with random SSM in the boost PFC circuit

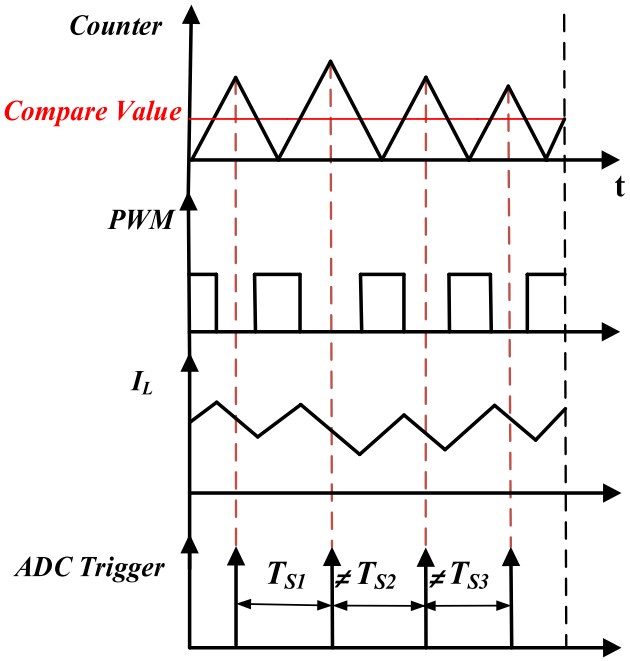

Fig. 5 Theoretical operating waveforms of random SSM with the variable sampling technique

However, when employing random SSM, the sensed current no longer represents the average current, because the sampled point in the inductor current changes over time. As noted in [19], attaining the average current when the switching frequency dithers requires the variable sampling to be synchronized with the PWM carrier.

Although variable sampling helps align the sampling period under the fluctuating operation induced by random SSM, current errors exist between the sampled current and the actual average current. This is because the variable sampled current only represents the average current limited to the negative slope of the instantaneous current waveforms. However, the errors are small enough to obtain low THD and high PF compared with the fixed sampling technique.

3.2 Proposed random SSM algorithm

In pseudo-random modulation, random numbers are commonly generated using the rand() function defined in the standard library header < stdlib.h > . It can generate random numbers between 0 to RAND_MAX (32,767). However, additional processes are required to employ random SSM in boost PFC. Since excessively large frequency steps can yield instability, the maximum value of the step frequency should be limited to guarantee the stable operation of boost PFC.

Figure 6 illustrates the flowchart of the proposed random SSM algorithm. The maximum magnitude of the step frequency and the range of the available switching frequency are initially selected. In this case, Δf is selected as the maximum step frequency magnitude based on experimental results, where the typical step frequency in pseudo-random modulation is approximately 3–6% of the center frequency [20, 21]. The algorithm determines whether the permissible range for the subsequent switching frequency is higher than the maximum step frequency by comparing the current switching frequency with the predefined minimum and maximum frequency. A normalized random value α is subsequently generated using the following equation:

$$\alpha = rand()/RANDMAX \tag{4}$$

After generating α, the step frequency f_{var} is calculated using the following equation, yielding the next randomized switching frequency when it is added to the current frequency, as follows:

$$f_{\text{var}} = x_l + \alpha \times (x_h - x_l) \tag{5}$$

where x_l and x_h are the lower and upper boundary of f_{var}.

3.3 Parameter selections of random SSM

In the discussions in Sect. 2.1, increasing the modulation index can achieve high EM noise mitigation performance. However, there are limitations to increasing Δf. CCM operation under the minimum frequency should be guaranteed. In addition, when the harmonic component increases, the bandwidth of adjacent harmonics can be overlapped. The harmonic bandwidth employing SSM, which shows the sum of right and left bandwidths of the n^{th} and $(n+1)^{\text{th}}$ harmonics, can be analyzed as follows:

$$B_{sum} = \frac{1}{2}(B_n + B_{n+1}) = (2n+1)\Delta f_s + 2f_m \tag{6}$$

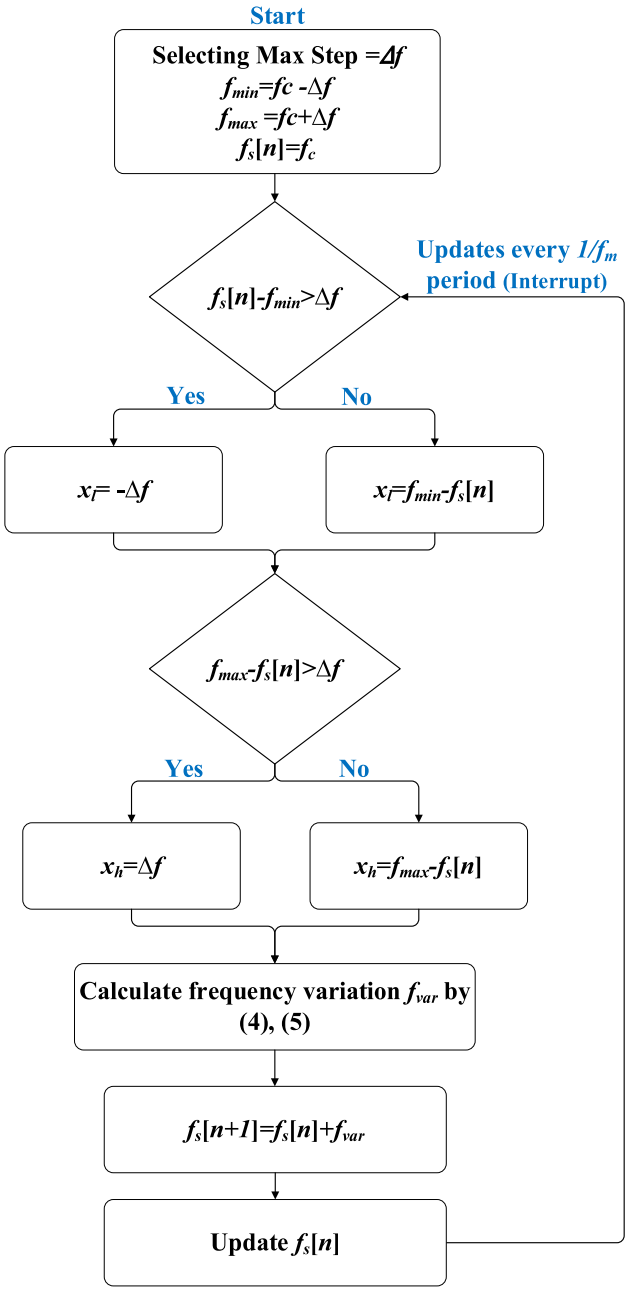

Fig. 6 Flowchart of the proposed random SSM algorithm

where B_n is the bandwidth of the nth harmonic, B_{n+1} is the (n + 1)th harmonic and B_{sum} is the sum of the right and left bandwidths of the nth and (n + 1)th harmonics, respectively. When B_{sum} is higher than f_s, overlap occurs, and the mitigation performance decreases significantly. Therefore, an adequate Δf should be selected based on high mitigation performance and to prevent the overlap bandwidth in the targeted frequency band.

The choice of f_m is constrained by the resolution bandwidth (RBW) of the EMI analyzer. When the RBW exceeds f_m, frequency dithering cannot be fully captured in the EMI analyzer, degrading EM noise mitigation performance. However, selecting a high value of f_m results in low m_f, leading to poor mitigation performance. Optimal EM noise mitigation performance is achieved when f_m is equal to the RBW under periodic SSM. However, for random SSM, the frequency is constant for each captured window under the above condition. To accommodate these constraints, f_m should exceed the RBW, but remain sufficiently low to sustain a high value of m_f [17].

To target the band A region, where the frequency band is 9 kHz to 150 kHz and the RBW of the EMI receiver is 200 Hz, f_m has been set as 1 kHz. To prevent overlap of the sidebands of the harmonic components in the region of the targeted EMI band, Δf has been set to 3 kHz. From (6), the sideband overlap occurs at the 6th harmonic, which is higher than the targeted frequency band. The selected SSM parameters yield a modulation index of 3, resulting in approximately 9.5 to 12 dB of EM noise mitigation. The inductor ripple ratio over the peak current is 26.33% at the minimum operating frequency, ensuring CCM operation.

Table 1 Design specifications of the prototype circuit

Parameters		Components	
V_{in}	220 Vac/60 Hz	D_B	RFUH20TF6S
V_o	380 V	S_1	C3M0015065K
L_B	700 uH	L_B	WE-TORPFC 760801321
C_x	100 nF	C_x	B32922C3104K289
C_o	660 uF (330uF × 2)	C_o	B43644A5337M000
f_{center}	37 kHz		
Δf	3 kHz		
f_m	1 kHz		

4 Simulation and experimental results

Simulations and experiments have been conducted to verify the effectiveness of random SSM with a 1.4 kW CCM boost PFC prototype employing the variable-sampling technique. Table 1 shows the design spec of the boost PFC and SSM parameters used in the simulations and experiments.

4.1 Simulation results

Figure 7 shows comparisons of the fixed and variable sampling techniques using PSIM simulation software. In Fig. 7a, the conventional fixed sampling technique does not produce current distortion without SSM. However, in Fig. 7b, severe distortions are produced in the input current when random SSM is employed. When the variable sampling technique is applied to PFC employing SSM, the input current distortions no longer occur. In Fig. 7a, the THD is measured as

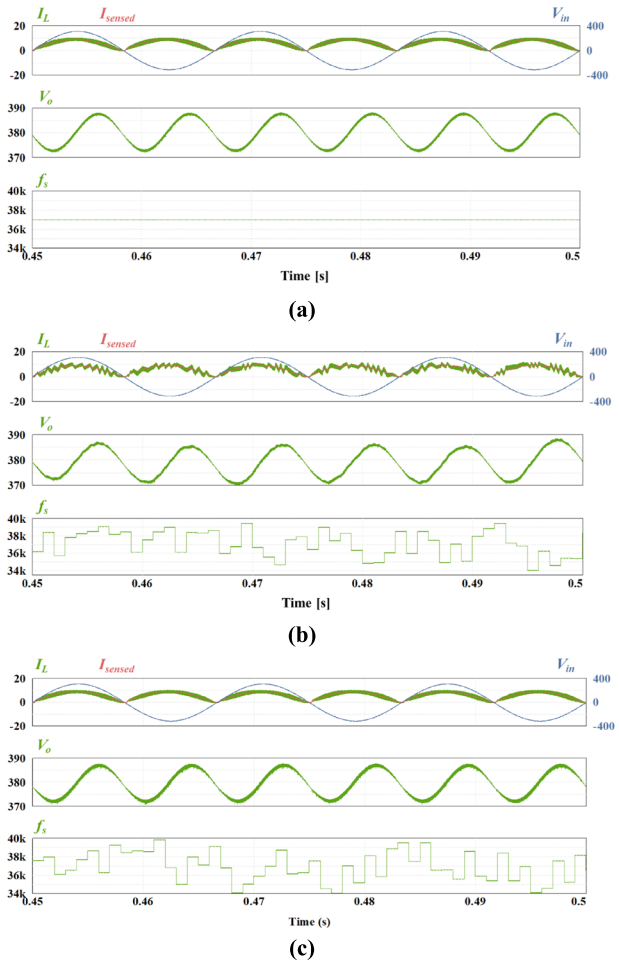

Fig. 7 Simulation waveforms under steady-state operation: **a** without SSM; **b** random SSM with fixed sampling; **c** random SSM with variable sampling

10.34% with a voltage ripple of 16.15 V, whereas Fig. 7b shows a measured THD of 20.09% with an 18.46 V voltage ripple. In Fig. 7c, the THD is measured as 12.81% with an output voltage ripple of 16.18 V. These results demonstrate that the variable sampling technique effectively mitigates the current distortions induced by random SSM, achieving a notable reduction in the THD while maintaining voltage ripple performance close to that of the conventional fixed sampling method.

4.2 Experimental results

Figure 8 shows the experimental setup of a 1.4 kW boost PFC circuit prototype, including a Texas Instruments TMS320F28379D digital controller, an EMCIS FFT-3010 EMI analyzer, an EMCIS EA-2100 common mode/differential mode noise separator, and an EMCIS LN2-16N line impedance stabilization network. The line impedance stabilization network (LISN) is connected to the ground plane

Fig. 8 Experimental setup of the 1400-W boost PFC converter

and provides measurements of the conducted noise with the ground plane as a reference. In addition, a YOKOGAWA WT5000 power analyzer measures the efficiency and current harmonic components of the prototype circuit.

Figure 9 shows experimental waveforms of the boost PFC prototype circuit operating at the rated power of 1.4 kW. When operating at a fixed frequency of 37 kHz, the output voltage ripple is 22.5 V, and the current THD is 5.78%. In contrast, when random SSM is applied to the boost PFC circuit with the variable sampling technique, the output voltage ripple is 21.52 V, and the current THD is 5.962%.

Due to severe input current distortions, the conventional fixed sampling method cannot be experimentally verified.

Figure 10 shows the experimentally measured THD, power factor, and efficiency under different loads. Conventional fixed-frequency operation shows 5.787% THD at the full load and 11.48% THD at the light load, whereas the proposed method shows 5.962% THD at the full load and 13.2% THD at the light load.

The difference in THD is only 0.175% at the full load. At the light-load, the THD increases 1.72%. This is mainly

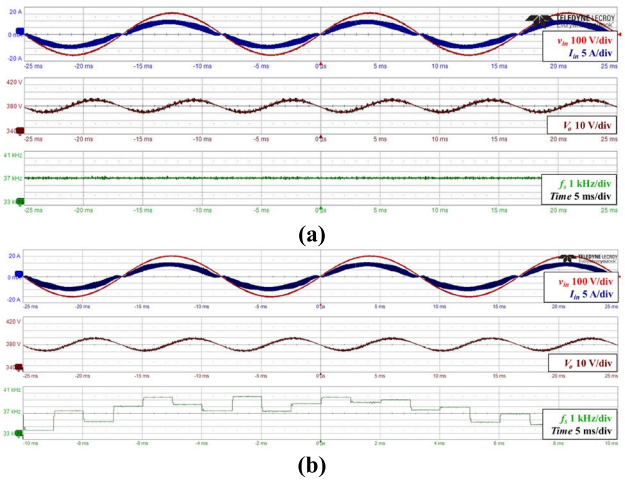

Fig. 9 Experimental waveforms under steady-state operation: **a** without SSM; **b** random SSM with variable sampling

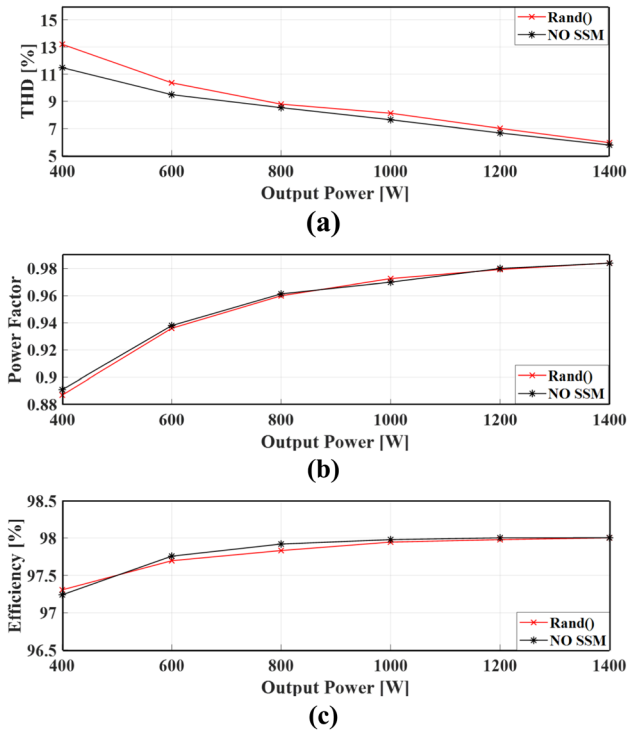

Fig. 10 Experimental results according to load conditions: **a** input current THD; **b** power factor; **c** efficiency

Table 2 Measured THD as a function of output load

	w/o SSM	w/random SSM
1400 W	5.787%	5.962%
1200 W	6.677%	7.012%
1000 W	7.641%	8.123%
800 W	8.533%	8.791%
600 W	9.488%	10.361%
400 W	11.48%	13.2%

due to the expansion of the DCM region in the line cycle, which leads to a heightened dependency on the switching frequency. The measured THD values are summarized in Table 2. In terms of efficiency, the difference between no SSM and random SSM is mostly around 0.2%, indicating a slight reduction in efficiency under random SSM operation (Table 3).

Figure 11 shows the measured total EM noise in the band A region (9 kHz ~ 150 kHz). The highest EM noise

Table 3 Experimental results of measured EM noise (dBμV)

	37 kHz	74 kHz	111 kHz
w/o SSM	128.71	121.4	121.39
w/random SSM	118.98	110.73	110.17

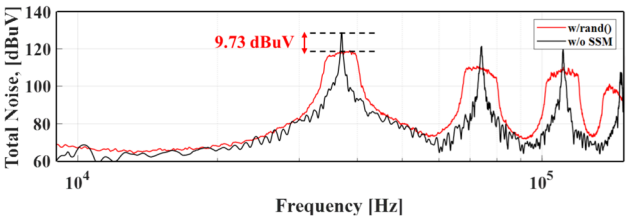

Fig. 11 Measurement data of conducted emission EM noise in the band A region

peak occurs at the switching frequency and its high-order harmonics when the converter operates at a fixed frequency. However, when random SSM is applied to the PFC circuit, EM noise mitigation performance of 9.73 dB at 37 kHz, 10.67 dB at 97 kHz, and 11.02 dB at 111 kHz are obtained. Employing SSM with the proposed method can reduce EM noise at the switching frequency and its harmonics with high cost-effectiveness while minimizing the impact on power quality and efficiency.

5 Conclusion

This article proposes a random SSM method using a variable sampling technique for a boost PFC circuit operating in the CCM. The proposed approach achieves significant EM noise reduction with minimal side effects. The variable sampling technique, synchronized with dynamically changing switching frequencies in random SSM, minimizes the measurement error between the sampled current and the actual average current. Compared with conventional fixed-frequency operation, the proposed random SSM with the variable sampling technique results in only a marginal increment in THD, 0.175% at full load and 1.72% at light load conditions while achieving an EM noise reduction of 9.73 dB at the center switching frequency.

Acknowledgements This work was supported by the National Research Foundation of Korea (NRF) grant funded by the Korea government (MIST) (No. RS-2024-00337108).

Funding Open Access funding enabled and organized by Ulsan National Institute of Science and Technology (UNIST). National Research Foundation of Korea, RS-2024-00337108, Jeehoon Jung

Data availability The datasets generated and analyzed during the current study are available from the corresponding author on reasonable request.

Declarations

Conflict of interest On behalf of all authors, the corresponding author states that there are no competing interests.

References

1. Kwon, M.J., Kang, S.H., Hwang, Y.S., et al.: Analysis and hardware implementation of induction-heating cooktops for maximizing usability and user convenience. J. Electr. Eng. Technol. **20**, 319–332 (2025)
2. Park, T.H., Lee, W.C.: Research on DC-link ripple voltage compensation for single-phase photovoltaic system by frequency analysis. J. Electr. Eng. Technol. **19**, 5201–5209 (2024)
3. Cho, J., Kim, S., Kim, Y., Yea, J., Han, B.: Bridgeless totem-pole resonant single-power-conversion PFC converter. IEEE Trans. Power Electron. **39**(11), 15257–15268 (2024)
4. Zhu, H., Dongliang, L., Zhang, X., Qu, F.: Reliability of Boost PFC Converters with Improved EMI Filters. Electronics (2018). https://doi.org/10.3390/electronics7120413
5. Yang, Y., Huang, D., Lee, F.C., Li, Q.: Analysis and reduction of common mode EMI noise for resonant converters. Proc. IEEE Appl. Power Electron Con. Expo. (2014). https://doi.org/10.1109/APEC.2017.7930695
6. Xu, K., Vaisband, B., Sizikov, G., Li, X., Friedman, E.G.: EMI suppression with distributed LLC resonant converter for high-voltage VR-on-package. IEEE Trans. Compon. Packag. Manuf. Technol. **10**(2), 263–271 (2020)
7. Fu, D., Wang, S., Kong, P., Lee, F.C., Huang, D.: Novel techniques to suppress the common-mode EMI noise caused by transformer parasitic capacitances in DC–DC converters. IEEE Trans. Ind. Electron. **60**(11), 4968–4977 (2013)
8. Fei, C., Yang, Y., Li, Q., Lee, F.C.: Shielding technique for planar matrix transformers to suppress common-mode EMI noise and improve efficiency. IEEE Trans. Ind. Electron. **65**(2), 1263–1272 (2018)
9. Kchikach, M., Elhasnanoui, A., Zazi, K., and Qian Z. M.: The electromagnetic interference (EMI) affect on power supply of telecom equipment. Proc. Asia-Pac. Int. Symp. Electromagn. Compat. 83–86. (2010)
10. Zhou, M., et al.: Optimized separation method for conducted EMI noise based on Mardiguian network and common mode choke. J. Power Electron. **21**(1), 204–213 (2021)
11. Liu, J.K., Yao, X.D., Liu, H.L.: PWM harmonic cancellation of permanent magnet synchronous motor based on periodic spread spectrum modulation. J. Electr. En. Technol. **19**(1), 2413–2423 (2024)
12. Kim, J.H., Jung, Y.G.: Spreading power spectrum of an induction motor drive system by chaotic pulse width modulation method. J. Electr. Eng. Technol. **16**, 2685–2694 (2021)
13. Stepins, D.: An improved control technique of switching-frequency-modulated power factor correctors for low THD and high power factor. IEEE Trans. Power Electron. **31**(7), 5201–5214 (2016)
14. Lee, M., Lai, J.-S.: Spread-spectrum frequency modulation with adaptive three-level current scheme to improve EMI and efficiency of three-level boost DCM PFC. IEEE Trans. Power Electron. **36**(3), 2476–2480 (2021)
15. Pareschi, F., Setti, G., Rovatti, R., Frattini, G.: Practical optimization of EMI reduction in spread spectrum clock generators with application to switching DC/DC converters. IEEE Trans. Power Electron. **29**(9), 4646–4657 (2014)
16. Pareschi, F., Rovatti, R., Setti, G.: EMI reduction via spread spectrum in DC/DC converters: state of the art, optimization, and tradeoffs. IEEE Access **3**, 2857–2874 (2015)
17. Kim, M., Park, H.-P., Jung, J.-H.: Spread spectrum technique with random-linear modulation for EMI mitigation and audible noise elimination in IH appliances. IEEE Trans. Ind. Electron. **69**(8), 8589–8593 (2022)
18. Yao, K., Ruan, X., Mao, X., Ye, Z.: Variable-duty-Cycle control to achieve high input power factor for DCM boost PFC converter. IEEE Trans. Ind. Electron. **58**(5), 1856–1865 (2011)
19. Lai, Y.-S., Chang, Y.-T., Chen, B.-Y.: Novel random-switching pwm technique with constant sampling frequency and constant inductor average current for digitally controlled converter. IEEE Trans. Ind. Electron. **60**(8), 3126–3135 (2013)
20. Rice, J., Gehrke, D., and Segal, M.: Understanding noise-spreading techniques and their effects in switch-mode power applications. Proc. VDM. 1(1): 1. (2008)
21. Jaffe S.: The pros and cons of spread-spectrum implementation methods in buck regulators. Analog Design Journal, Texas Instruments. (2021)

Young-Joon Song was born in Changwon, South Korea, in 1998. He received his B.S. degree in Electrical Engineering from the Kyungpook National University, Daegu, South Korea, in 2023. He is currently working towards his M.S. degree in Electrical Engineering at the Ulsan National Institute of Science and Technology (UNIST), Ulsan, South Korea. His main research interests include spread spectrum modulations and AC/DC Converter.

Kyung-Wook Heo was born in Daegu, South Korea, in 1994. He received his B.S. degree in Electronic Engineering from the Kumoh National Institute of Technology, Gumi, South Korea, in 2019; and his Ph.D. degree in Electrical Engineering from the Ulsan National Institute of Science and Technology (UNIST), Ulsan, South Korea, in 2025. He is currently working at the Agency for Defense Development (ADD), Daejeon, South Korea. His main research interests include DC/DC resonant converters, bidirectional DC/DC converters, AC/DC and DC/AC converters for consumer and industrial applications, and power hardware-in-the-loop simulations.

Jun-Suk Lee was born in Seoul, South Korea, in 1997. He received his B.S. degree in Electrical and Electronic Engineering from the University of Ulsan, Ulsan, South Korea, in 2023. He is currently working under a M.S.-Ph.D. joint program in Electrical Engineering from the Ulsan National Institute of Science and Technology (UNIST), Ulsan, South Korea. His main research interests include resonant converters, induction heating systems, talkative power conversion, and spread spectrum modulations.

Sang-Yeop Kim was born in Ulsan, South Korea, in 1999. He received his B.S. degree in Electrical and Information Engineering from the Seoul National University of Science and Technology, Seoul, South Korea, in 2024. He is currently working towards his M.S. degree in Electrical Engineering at the Ulsan National Institute of Science and Technology (UNIST), Ulsan, South Korea. His main research interests include spread spectrum modulations, hardware-in-the-loop simulations, and hybrid transformers.

Jee-Hoon Jung was born in Suwon, South Korea, in 1977. He received his B.S. degree in Electrical Engineering and the M.S. and Ph.D. degrees in Electrical and Computer Engineering from the Department of Electronics and Electrical Engineering, Pohang University of Science and Technology (POSTECH), Pohang, South Korea, in 2000, 2002, and 2006, respectively. From 2006 to 2009, he was a Senior Research Engineer in the Digital Printing Division, Samsung Electronics Company Ltd., Suwon, South Korea. From 2009 to 2010, he was a Postdoctoral Research Associate with the Department of Electrical and Computer Engineering, Texas A&M University at Qatar, Doha, Qatar. From 2011 to 2012, he was a Senior Researcher in the Power Conversion and Control Research Center, HVDC Research Division, Korea Electrotechnology Research Institute (KERI), Changwon, South Korea. Since 2013, he has been involving as a faculty member in the Dept. of Electrical Engineering, Ulsan National Institute of Science and Technology (UNIST), Ulsan, South Korea, where he is presently working as a Professor. His current research interests include DC/DC, AC/DC, and DC/AC converters, switched-mode power supplies, digital control & signal processing algorithms, power conversion techniques for renewable energy, and real-time and power hardware-in-the-loop (HIL) simulations of renewable energy and power grids. Recently, he has been researching high-frequency power converters using wide bandgap (WBG) devices, bidirectional power converters for smart grids and EVs, advanced power control algorithms, spread spectrum modulations for reducing EM noises in various power converters, information-bearing noise communications for DC microgrids, induction heating techniques for home appliances & industrial applications, and partial power processing techniques applied to hybrid transformers. Dr. Jung is a Senior Member of the IEEE Power Electronics Society (PELS), the IEEE Industrial Electronics Society (IES), the IEEE Industry Applications Society (IAS), and the IEEE Power and Energy Society (PES). He had served as a Member of the Editorial Committee of the Korea Institute of Power Electronics (KIPE) and an Associate Editor for the IEEE Journal of Emerging and Selected Topics in Power Electronics. He has been an Asian liaison officer for the Industrial Power Converter Committee in the IEEE IAS, an editor for the Journal of Power Electronics (JPE), and a member of the Board of Directors of the KIPE.